Modeling of Active Control on KSTAR

Oksana Katsuro-Hopkins[1], S.A. Sabbagh[1], J.M. Bialek[1], H.K. Park[2], J.Y. Kim[3], K.-I. You[3], A.H. Glasser[4], L.L. Lao[5]

[1]Department of Applied Physics, Columbia University, New York, NY, USA

[2]Plasma Physics Laboratory, Princeton University, Princeton, NJ, USA

[3]Korea Basic Science Institute, Daejeon, Korea

[4]Los Alamos National Laboratory, Los Alamos, NM, USA

[5]General Atomics, San Diego, CA, USA

Workshop on Active Control of MHD Stability

November 18-20, 2007

Columbia University, New York, NY

Numerical design study to optimize advanced stability of KSTAR merging present experimental results & machine design

- Motivation
  - Design optimal global MHD stabilization system for KSTAR with application to future burning plasma devices

- Outline
  - Free boundary equilibrium calculations
  - Ideal stability operational space for experimental profiles
  - RWM stability and VALEN-3D modeling
  - Advanced feedback control algorithm and performance

*O.Katsuro-Hopkins at al., Nucl. Fusion **47** (2007) 1157-1165.

Korea Superconducting Tokamak Advanced Research will study steady-state advanced tokamak operation & technology

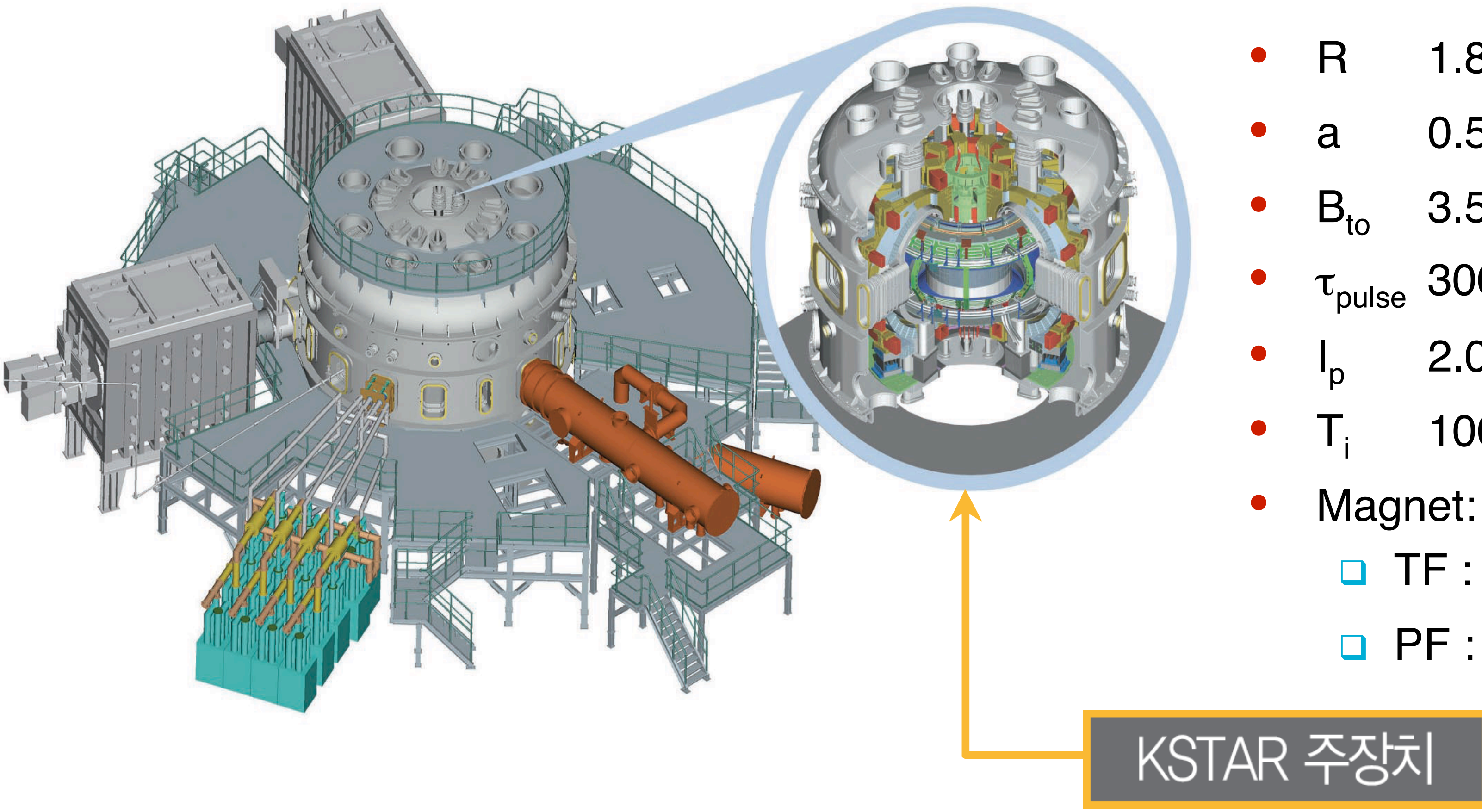

Parameters:

- R 1.8m
- a 0.5 m
- B_{to} 3.5 T
- τ_{pulse} 300 s
- I_p 2.0 MA
- T_i 100~300MC
- Magnet:
  - TF : Nb3Sn,
  - PF : NbTi

KSTAR configuration used in EFIT calculations

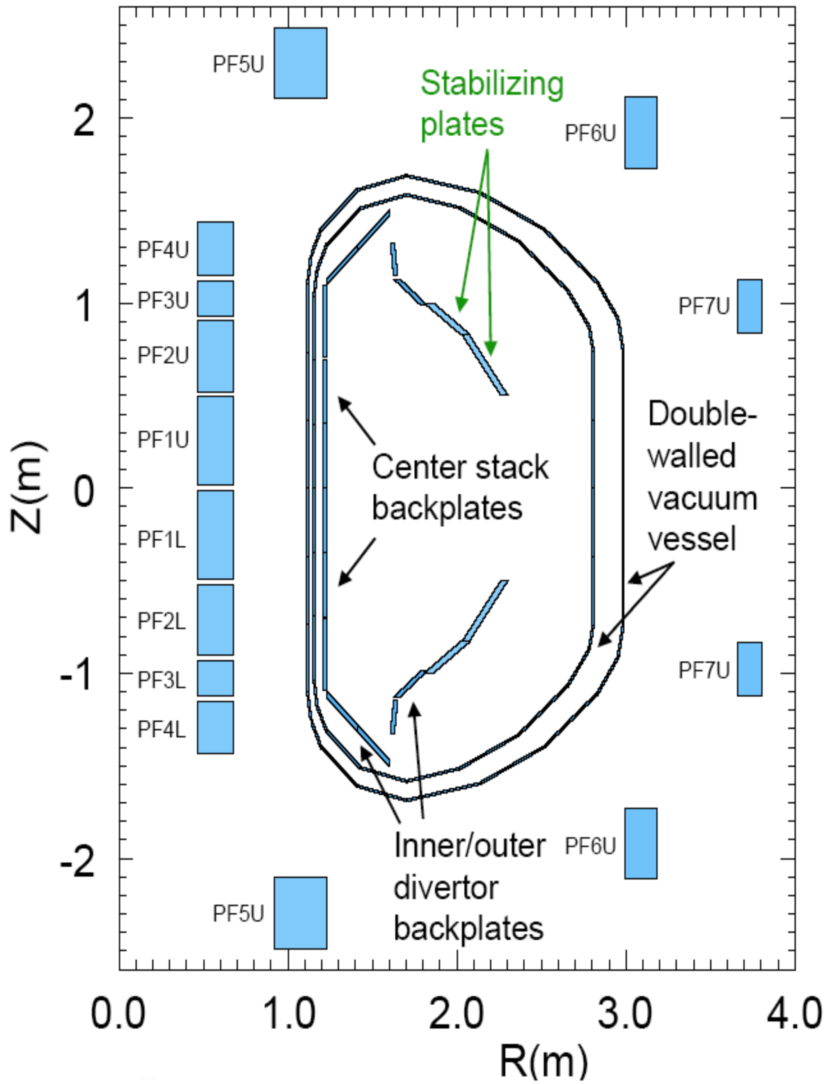

- EFIT industry-standard tool
  - Free-boundary equilibria
  - Expandable range of equilibria
- Data from KSTAR design drawings
- Passive stabilizers/vacuum vessel included.
  - Important for start up studies
  - Reconstructions during events that change edge current (e.g. ELMs)

Equilibrium variations produced to scan (l_i,β_n)

- Boundary shape
  - Free-boundary equilibria with high shaping κ~2,δ~0.8
  - Shaping coil currents constrained to machine limits
- Pressure profile
  - Generic "L-mode", edge p'=0
  - H-mode, modeled from DIII-D
- q profile
  - Monotonic to mild shear reversal with q_0>1 and (q_0-q_{min})<1
- Variations in (l_i,β_n) produced
  - $0.5 \leq l_i \leq 1.2$; $0.5 \leq \beta_n \leq 8.0$

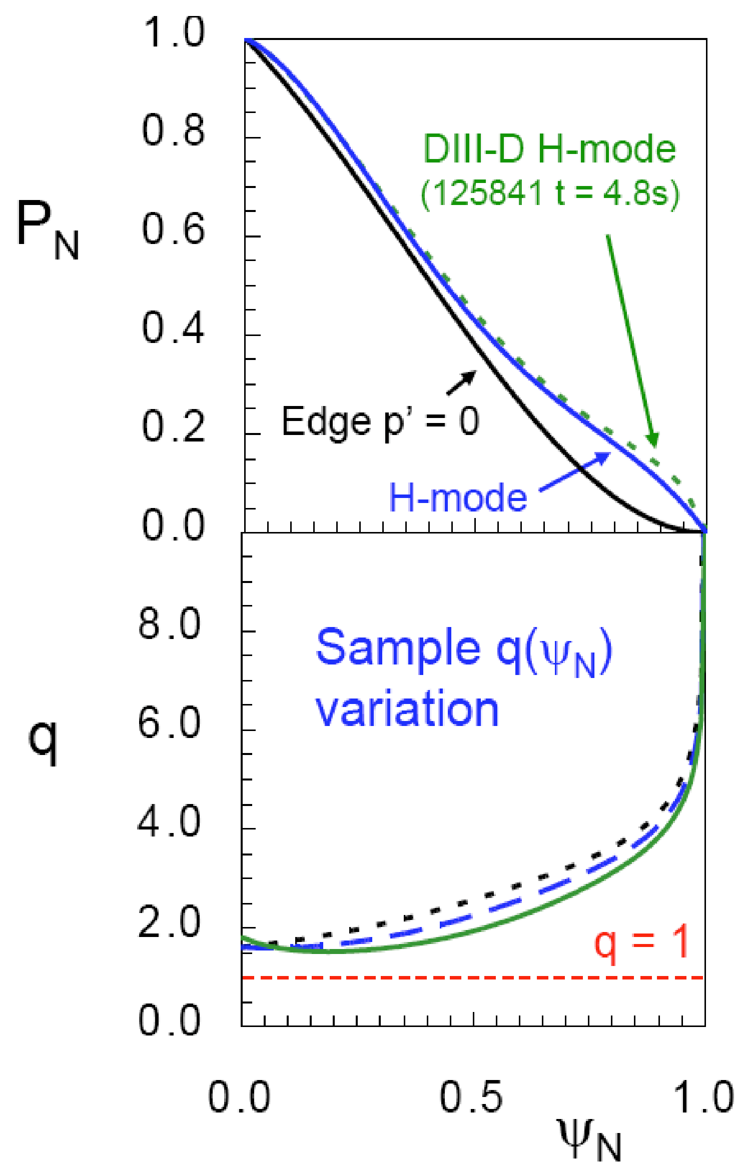

Ideal stability(DCON): conducting wall allows significant passive stabilization for n=1 H-mode pressure profile

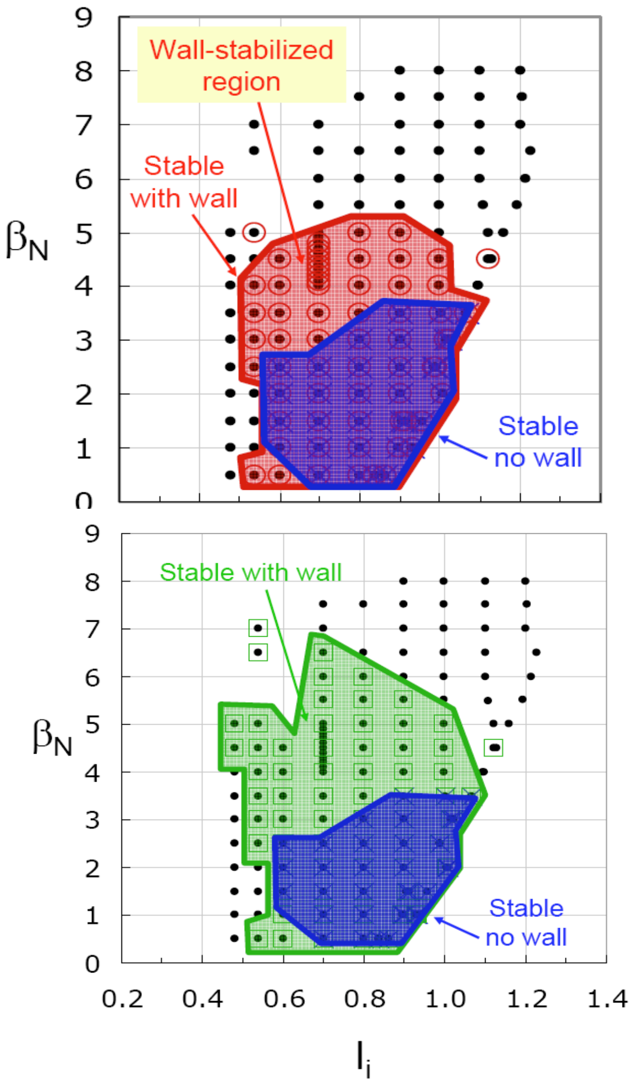

- "inner" wall used

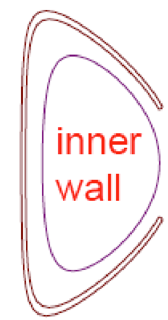

- Wall-Stabilized β_n is a factor of two greater then for equilibrium without wall at $l_i \sim 0.7$
- Wall-Stabilized β_n from DCON agrees with VALEN-3D value

- "outer" wall used

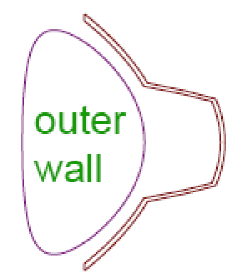

- Wall-Stabilized $\beta_n > 6.5$ (larger than the result using "inner" wall at $l_i \sim 0.7$)
- Optimistic, but does not agree with VALEN-3D. "Inner" wall is more realistic and should be used in DCON analysis

L-mode pressure profile has large n=1 stabilized region

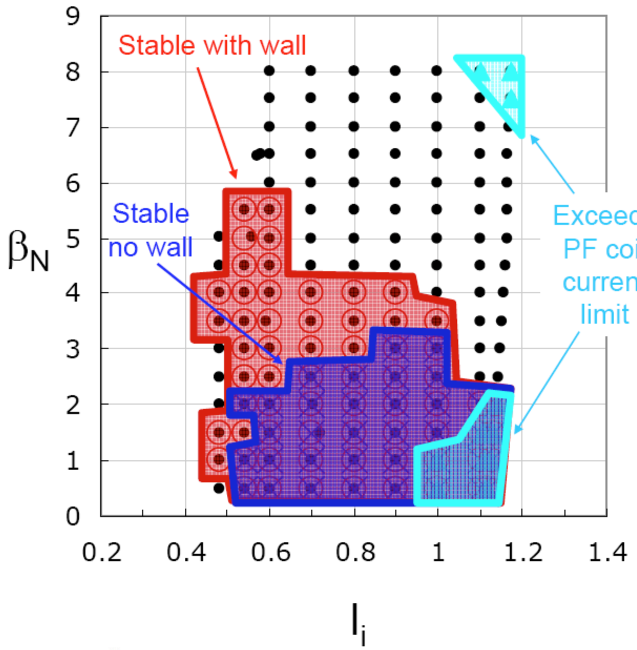

- "inner" wall used
- Wall-Stabilized region at lowest l_i (Unfavorable for n=0 stabilization)
- Possible difficulty to access with L-mode confinement.

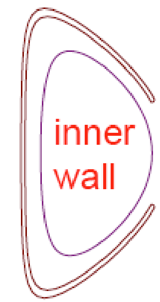

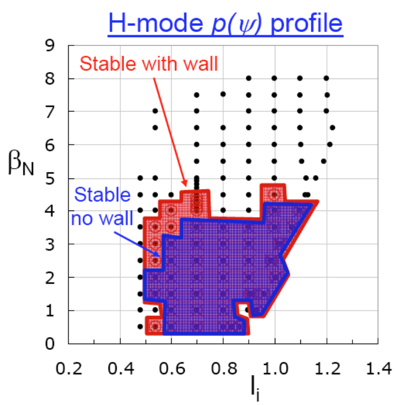

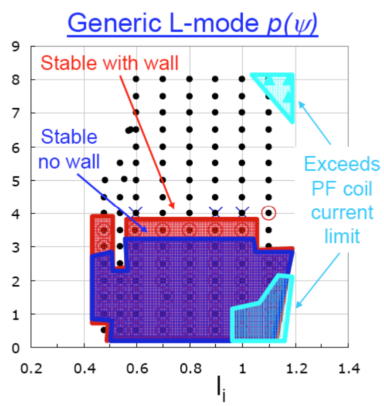

- **n=2 stability** has higher no-wall & lower with-wall limits than n=1 for H-mode and L-mode pressure profile
  - Internal n=2 modes were observed in NSTX during n=1 active RWM stabilization.

Conducting hardware, IVCC set up in VALEN-3D* based on engineering drawings

n=1 RWM passive stabilization currents

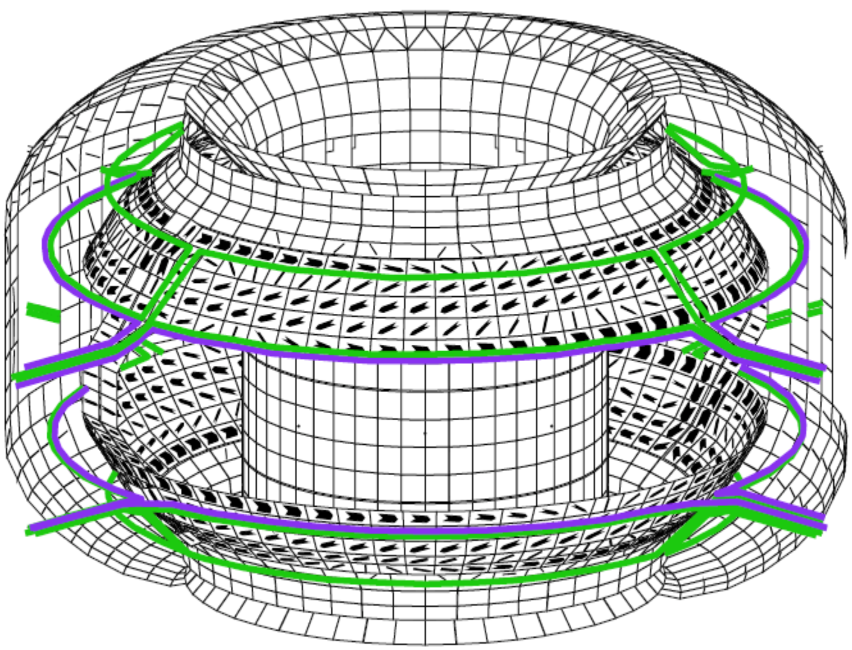

IVCC (RWM) control coils
(upper,middle,lower)

*Bialek J. et al 2001 Phys. Plasmas **8** 2170

- Conducting structures modeled
  - Vacuum vessel with actual port structure
  - Center stack back-plates
  - Inner and outer divertor back-plates
  - Passive stabilizer
  - PS Current bridge
- Stabilization currents dominant in PS
  - 40 times less resistive than nearby conductors.

VALEN 3-D code reproduces n=1 DCON β_n ideal wall limit

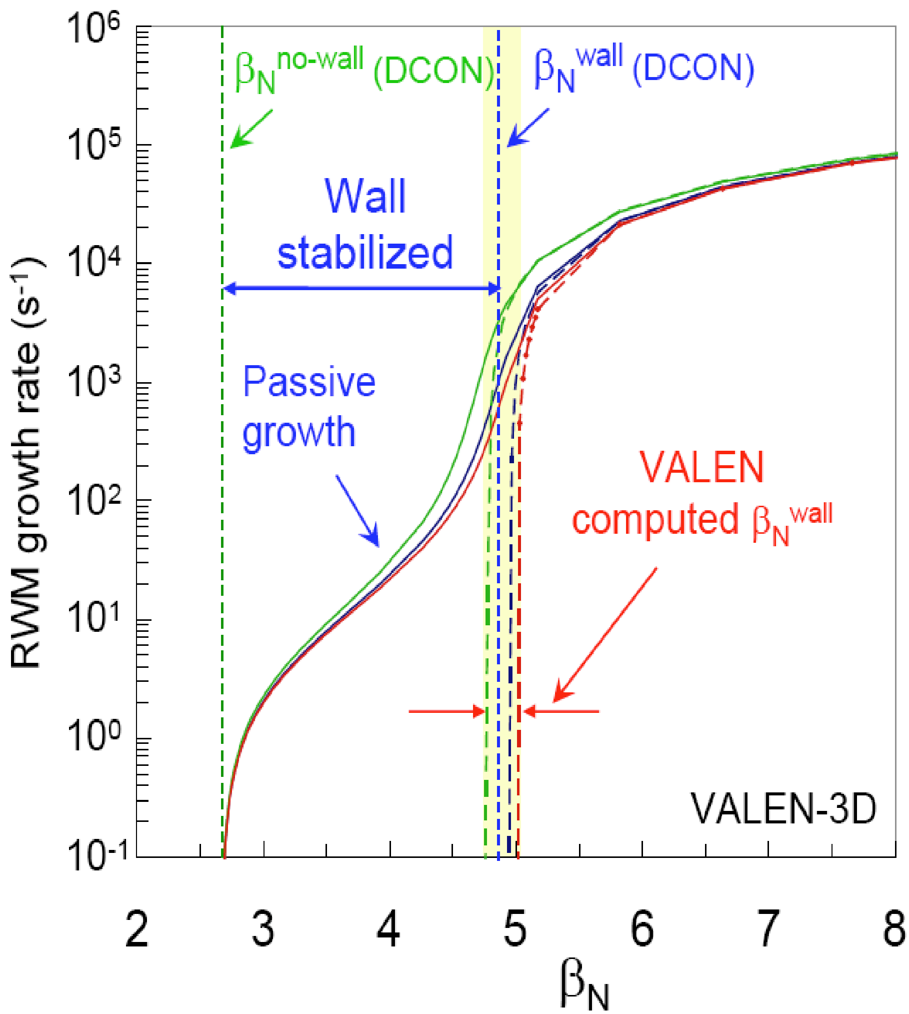

- Important cross-check VALEN-3D/DCON calibration
- Equilibrium β_n scan with l_i=0.7 H-mode pressure profile
- DCON n=1 β_n limits:
  - $\beta_n^{no-wall} = 2.6$
  - $\beta_n^{wall} = 4.8$
- VALEN-3D n = 1 β_n^{wall}
  - $4.77 < \beta_n^{wall} < 5.0$
  - Range generated by various RWM eigenfunctions from equilibria near $\beta_n = 5$.

IVCC allows active n=1 RWM stabilization near ideal wall.

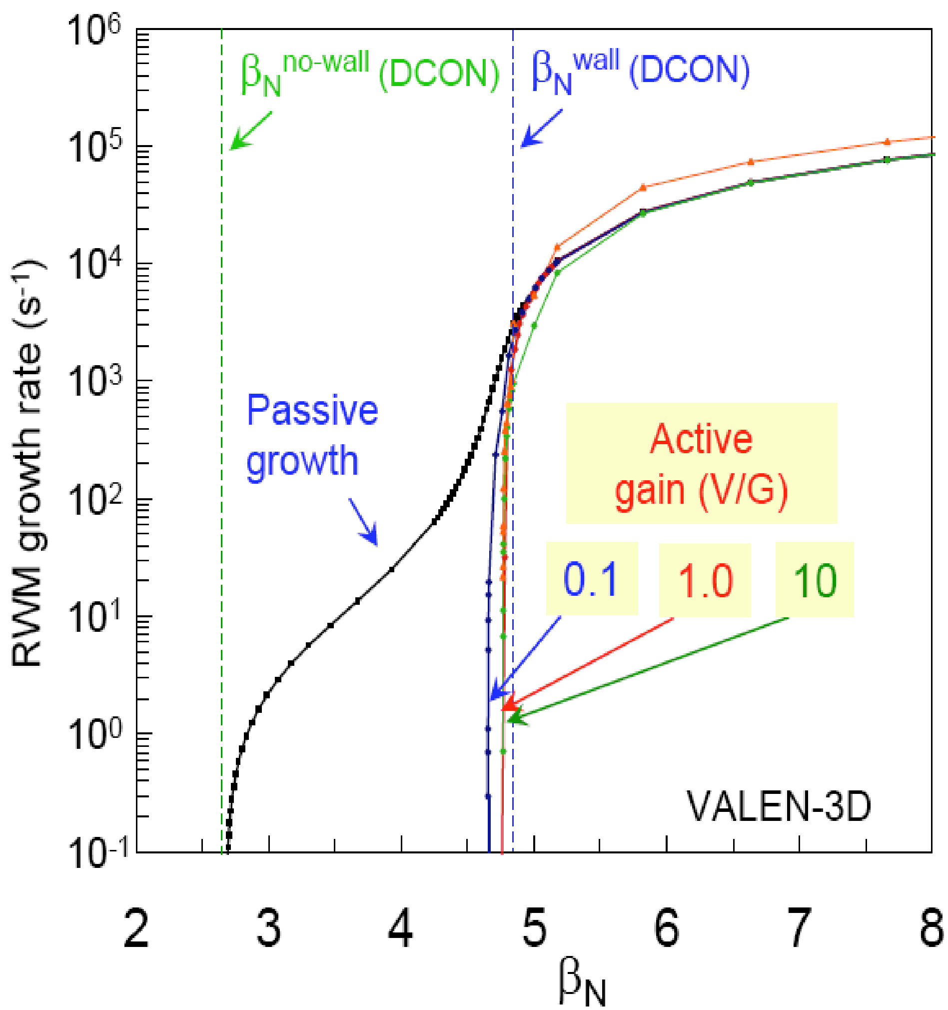

- Active n=1 RWM stabilization capability with

$$C_\beta = \frac{\beta_n - \beta_n^{no\ wall}}{\beta_n^{wall} - \beta_n^{no\ wall}} > 98\%$$

  - Optimal ability for mode stabilization
  - Mid-plane IVCC used
- Equilibrium β_n scan with l_i=0.7 H-mode pressure profile
- Computed β_n limits
  - $\beta_n^{no\text{-}wall}$ = 2.56
  - β_n^{wall} = 4.76

Power estimates bracket needs for KSTAR RWM control

Proportional gain controller

	C_β	White noise (1.6-2.0G RMS) (RMS values) I_{IVCC}(A)	V_{IVCC}(V)	P_{IVCC}(W)	NSTX 120047 ΔB_p sensors (RMS values) I_{IVCC}(A)	V_{IVCC}(V)	P_{IVCC}(W)
Unloaded IVCC L=10μH R=0.86mOhm L/R=12.8ms	80%	30	1.6	45	362	0.7	253
	95%	41	2.0	82	430	0.8	307
FAST IVCC circuit L=13μH R=13.2mOhm L/R=1.0ms	80%	20.9	1.56	30.0	1.9e3	24.9	62e3
	95%	28.3	1.78	50.6	9e3	119	1.8e6

Power estimates bracket needs for KSTAR RWM control

Proportional gain controller / **LQG controller**

(RMS values)

	C_β	White noise (1.6-2.0G RMS): I_{IVCC}(A)	V_{IVCC}(V)	P_{IVCC}(W)	NSTX 120047 ΔB_p sensors: I_{IVCC}(A)	V_{IVCC}(V)	P_{IVCC}(W)
Unloaded IVCC L=10μH R=0.86mOhm L/R=12.8ms	80%	30 / **29**	1.6 / **0.8**	45 / **24**	362	0.7	253
	95%	41 / **35**	2.0 / **0.9**	82 / **34**	430	0.8	307
FAST IVCC circuit L=13μH R=13.2mOhm L/R=1.0ms	80%	20.9	1.56	30.0	1.9e3	24.9	62e3
	95%	28.3	1.78	50.6	9e3	119	1.8e6

- Initial results using advanced Linear Quadratic Gaussian (LQG) controller yield factor of 2 power reduction for white noise.
- LQG controller consists of two steps:
  - Balanced Truncation of VALEN state-space for fixed β_n
  - Optimal controller and observer design based on the reduced order system

State-space control approach may allow superior feedback performance

- VALEN circuit equations after including plasma stability effects the fluxes at the wall, feedback coils and plasma are given by

$$\vec{\Phi}_w = \overleftrightarrow{L}_{ww} \cdot \vec{I}_w + \overleftrightarrow{L}_{wf} \cdot \vec{I}_f + \overleftrightarrow{L}_{wp} \cdot I_d$$

$$\vec{\Phi}_f = \overleftrightarrow{L}_{fw} \cdot \vec{I}_w + \overleftrightarrow{L}_{ff} \cdot \vec{I}_f + \overleftrightarrow{L}_{fp} \cdot I_d$$

$$\Phi_p = \overleftrightarrow{L}_{pw} \cdot \vec{I}_w + \overleftrightarrow{L}_{pf} \cdot \vec{I}_f + \overleftrightarrow{L}_{pp} \cdot I_d$$

- Equations for system evolution are given by

$$\begin{pmatrix} \overleftrightarrow{\mathcal{L}}_{ww} & \overleftrightarrow{\mathcal{L}}_{wf} & \overleftrightarrow{\mathcal{L}}_{wp} \\ \overleftrightarrow{\mathcal{L}}_{fw} & \overleftrightarrow{\mathcal{L}}_{ff} & \overleftrightarrow{\mathcal{L}}_{fp} \\ \overleftrightarrow{\mathcal{L}}_{pw} & \overleftrightarrow{\mathcal{L}}_{pf} & \overleftrightarrow{\mathcal{L}}_{pp} \end{pmatrix} \cdot \frac{d}{dt} \begin{pmatrix} \vec{I}_w \\ \vec{I}_f \\ I_d \end{pmatrix} = \begin{pmatrix} \overleftrightarrow{R}_w & 0 & 0 \\ 0 & \overleftrightarrow{R}_f & 0 \\ 0 & 0 & \overleftrightarrow{R}_d \end{pmatrix} \cdot \begin{pmatrix} \vec{I}_w \\ \vec{I}_f \\ I_d \end{pmatrix} + \begin{pmatrix} \vec{0} \\ \vec{V}_f \\ 0 \end{pmatrix}$$

- In the state-space form

$$\dot{\vec{x}} = \overleftrightarrow{A}\vec{x} + \overleftrightarrow{B}\vec{u}$$
$$\vec{y} = C\vec{x}$$

where $\vec{x} = \left(\vec{I}_w \ \vec{I}_f \ I_d\right)^T; \quad \overleftrightarrow{A} = -\overleftrightarrow{L}^{-1} \cdot \overleftrightarrow{R}; \quad \overleftrightarrow{B} = \overleftrightarrow{L}^{-1} \cdot \overleftrightarrow{I}_{cc}; \quad \vec{u} = \vec{V}_f$

& measurements $\vec{y} = \vec{\Phi}_s$ are sensor fluxes. State-space dimension ~1000 elements!

- Classical control law with proportional gain defined as $\vec{u} = -\overleftrightarrow{G}_p \vec{y}$

Balanced Truncation significantly reduces VALEN state-space

$$\dot{\vec{x}} = \overleftrightarrow{A}\vec{x} + \overleftrightarrow{B}\vec{u}$$
$$\vec{y} = C\vec{x}$$

- Measure of system controllability and observability is given by controllability and observability grammians for stable Linear Time-Invariant (LTI) Systems

$$\Gamma_c = \int_0^\infty e^{A\tau} B B^T e^{A^T\tau} d\tau \qquad \Gamma_o = \int_0^\infty e^{A^T\tau} C^T C e^{A\tau} d\tau$$

- Can be calculated by solving continuous-time Lyapunov equations:

$$A\Gamma_c + \Gamma_c A^T + BB^T = 0 \qquad A^T\Gamma_o + \Gamma_o A + C^T C = 0$$

- Balanced realization exists for every controllable & observable system

$$\Gamma_c = \Gamma_o = \begin{pmatrix} \sigma_1 & 0 & 0 \\ 0 & \ddots & 0 \\ 0 & 0 & \sigma_n \end{pmatrix}, \qquad \sigma_i > \sigma_j \text{ for } i > j$$

- Balanced truncation reduces VALEN state space from several thousand elements to ~15 or less

$$\vec{x} = (\vec{x}_1, \vec{x}_2)^T \qquad \begin{pmatrix} \dot{\vec{x}}_1 \\ \dot{\vec{x}}_2 \end{pmatrix} = \begin{pmatrix} A_{11} & A_{12} \\ A_{21} & A_{22} \end{pmatrix} \begin{pmatrix} \vec{x}_1 \\ \vec{x}_2 \end{pmatrix} + \begin{pmatrix} B_1 \\ B_2 \end{pmatrix} \vec{u}$$

$$\vec{y} = (C_1 \;\; C_2) \begin{pmatrix} \vec{x}_1 \\ \vec{x}_2 \end{pmatrix} + D\vec{u}$$

HSV spectrum of KSTAR VALEN state-space suggests a reduction of stable part of the system to just 2 balanced states

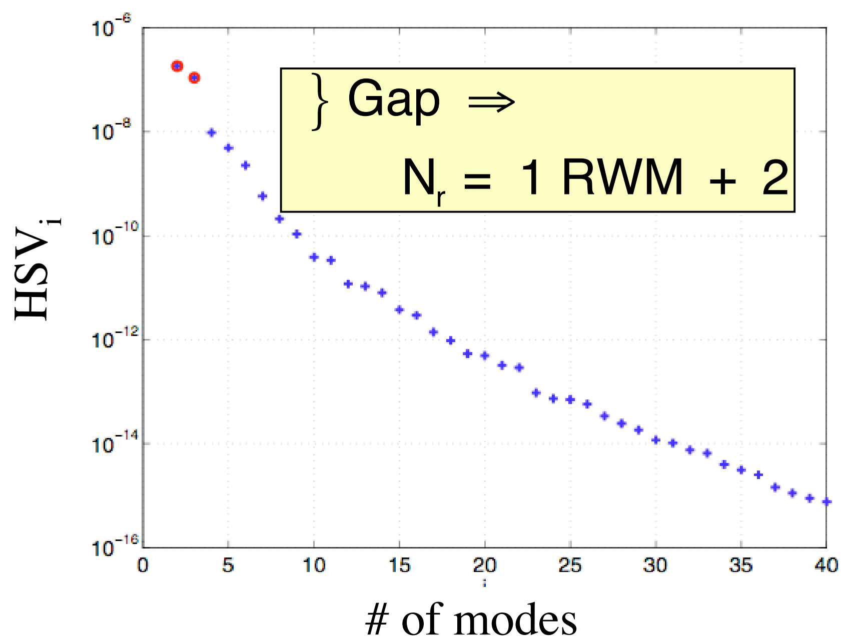

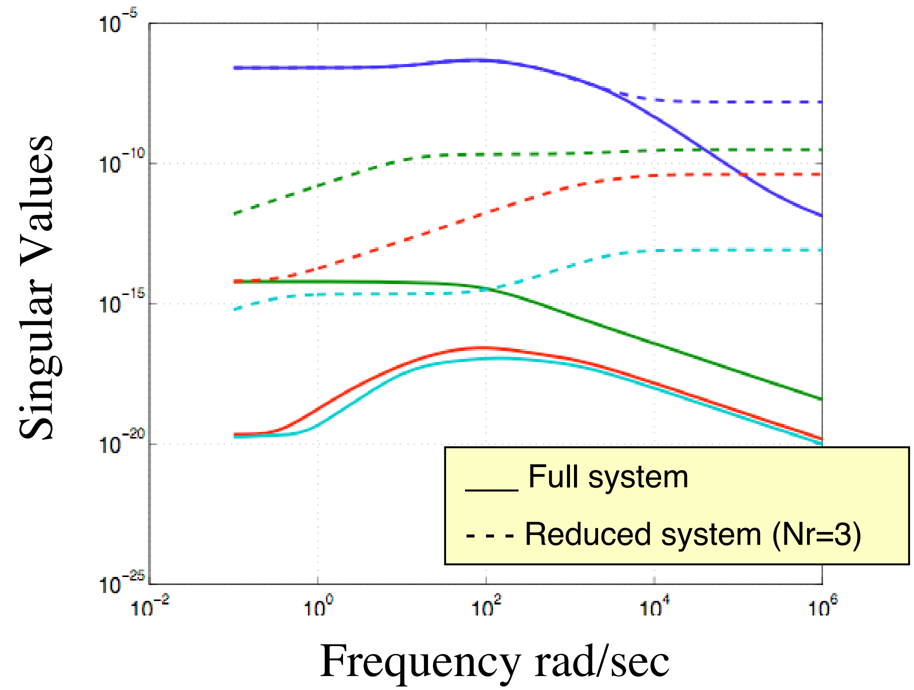

- LQG controller uses **4 central IVCC & 16 mid-plane poloidal sensors**
- Clear gap in HSV spectrum
- Largest SV includes the **full system frequency response up to an RWM passive growth rate**.

Closed System Equations with Optimal Controller and Optimal Observer based on Reduced Order Model

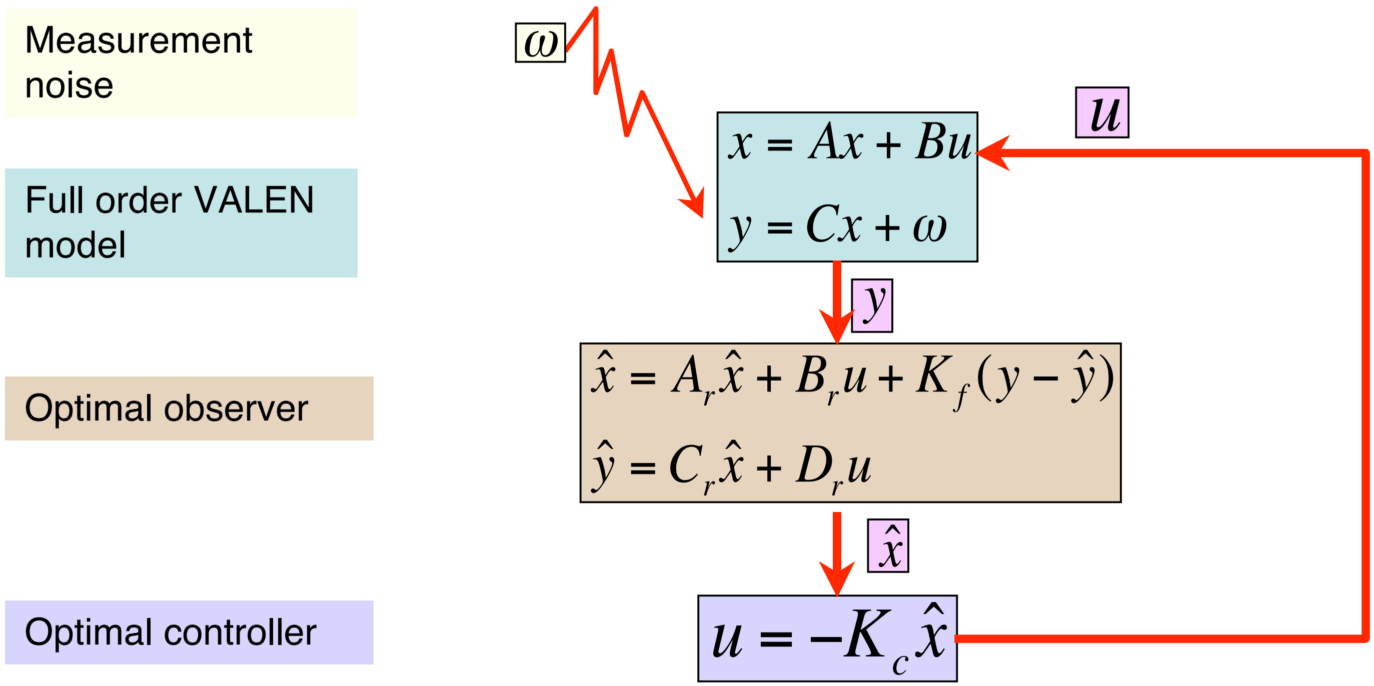

$$\begin{pmatrix} \dot{x} \\ \dot{\hat{x}} \end{pmatrix} = \begin{pmatrix} A & -BK_cC_r \\ K_fC & F \end{pmatrix} \begin{pmatrix} x \\ \hat{x} \end{pmatrix} + \begin{pmatrix} 0 \\ K_f \end{pmatrix} \omega$$

$$F = A_r - K_fC_r - (B_r - K_fD_r)K_cC_r$$

⇐ Closed loop continuous system allows to

- Test if Optimal controller and observer stabilizes original full order model
- Verify robustness with respect to β_n
- Estimate RMS of steady-state currents, voltages and power

Advanced controller methods planned to be tested on **NSTX** with future application to KSTAR

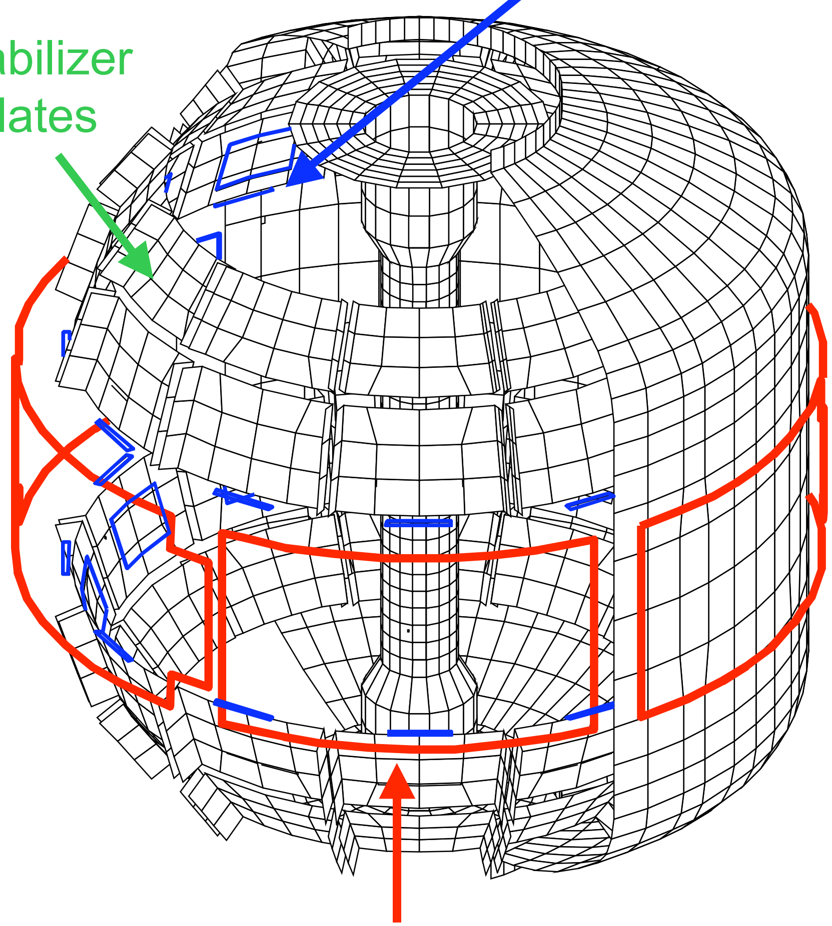

- VALEN NSTX Model includes
  - Stabilizer plates for kink mode stabilization
  - External mid-plane control coils closely coupled to vacuum vessel
  - Upper Bp sensors in actual locations
  - Compensation of control field from sensors
  - Experimental Equilibrium reconstruction (including MSE data)
- Present control system on NSTX uses Proportional Gain

Advanced control techniques suggests significant feedback performance improvement for NSTX up to β_n / β_n^{wall} = 95%

- Classical proportional feedback methods
  - VALEN modeling of feedback systems agrees with experimental results
  - RWM was stabilized up to β_n = 5.6 in experiment.
- Advanced feedback control may improve feedback performance
  - Optimized state-space controller can stabilize up to C_β=87% for upper Bp sensors and up to C_β=95% for mid-plane sensors
  - Uses only15 modes for optimal observer and controller design

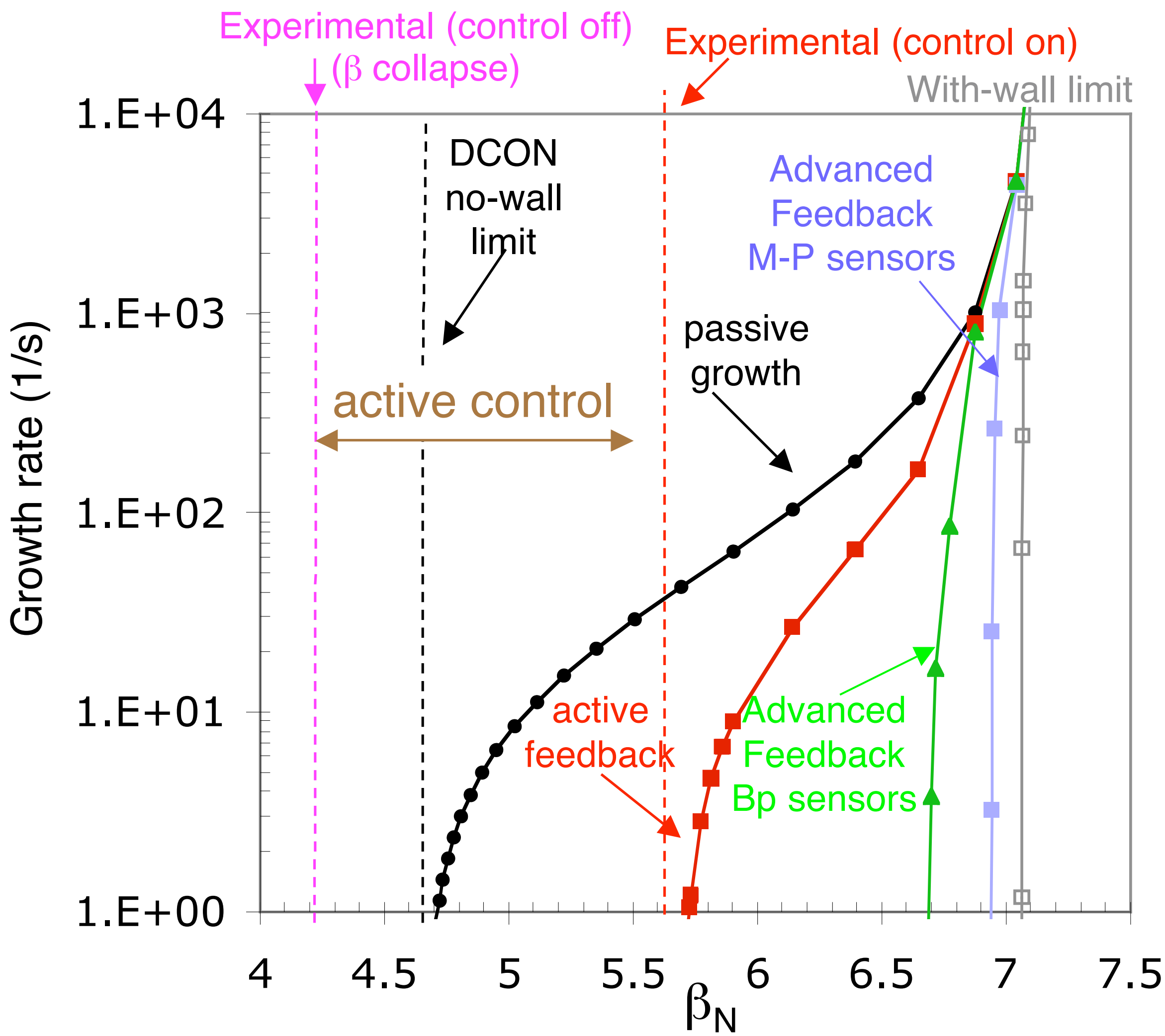

Next steps and future work on the KSTAR stability analysis

- Expand equilibrium / ideal stability analysis as needed
  - Collaborate on equilibrium reconstructions of first plasmas
- Closer definition of RWM control system circuit by interaction with KSTAR engineering team
- Improved noise model for KSTAR sensor noise
- LQG controller with plasma rotation for KSTAR
- LQG controller tests on NSTX with application to KSTAR RWM control system design
- Critical latency testing for KSTAR RWM control

KSTAR is capable of producing long-pulse, high β_n stability research

- Machine designed to run high β_n plasmas with low l_i and significant plasma shaping capability
- Large wall-stabilized region to kink/ballooning modes with $\beta_n / \beta_n^{no\text{-}wall} = 2$ at highest β_n predicted for the device
  - Co-directed NBI, passive stabilizers allow kink stabilization
- Active IVCC mode control system provide strong RWM control
  - IVCC design allows active $n = 1$ RWM stabilization at very high $C_\beta > 98\%$
- Fast IVCC circuit for stabilization is possible at reasonable power levels

Optimal controller and observer based on reduced order VALEN model reduce power and achieve higher β_n

Controller: $u = -K_c \hat{x}$

Minimize Performance Index: $J = \int_t^T \left(\vec{\hat{x}}'(\tau) Q_r(\tau) \vec{\hat{x}}(\tau) + \vec{u}'(\tau) R_r(\tau) \vec{u}(\tau) \right) d\tau \rightarrow \min$

Q_r, R_r - state and control weighting matrix,

Controller gain for the steady-state can be calculated as $K_c = R^{-1} B_r^T S$

where S is solution of the controller

Riccati equation $SA_r + A_r^T S - SB_r R_r^{-1} B_r^T S + Q_r = 0$

Observer: $\dot{\hat{x}} = A_r \hat{x} + B_r u + K_f (y - C_r \hat{x})$

Minimize error covariance matrix $E\{(x - \hat{x})(x - \hat{x})^T | y(\tau), \tau \le t\} \rightarrow \min$

where $K_f = PC'W^{-1}$ is Kalman Filter gain and

P is solution of observer

Riccati equation $A_r P + PA_r^T - PC_r^T W^{-1} C_r P + V^T = 0$

V, W plant and measurement noise covariance matrix.

Noise on RWM sensors sets control system power

- Gaussian white noise
  - ~1.5Gauss RMS, based on noise in DIII-D RWM B_p sensors
  - Minimum estimate of control power consumption
    - Perfect response to RWM
    - No other coherent modes

- Experimental sensor input
  - NSTX B_p sensor during RWM active stabilization
  - Maximum estimate of control system power consumption
    - DC offset from resonant field amplification; stray field from passive plate currents
    - The $\Delta B/B_0$ larger in ST than at higher apsect ratio